Received: 3 May 2022 | Revised: 27 August 2022 | Accepted: 5 September 2022

IET Microwaves, Antennas & Propagation

DOI: 10.1049/mia2.12299

The Institution of Engineering and Technology WILEY

ORIGINAL RESEARCH

Compact UHF RFID balun-like integrated tag antenna for long range detection of water bottles

Manoj Garg[1] | Ashwani Sharma[1] | Ignacio J. Garcia Zuazola[2] | Arjit Gupta[1]

[1]Electrical Engineering Department, Indian Institute of Technology Ropar, Punjab, India

[2]School of Computing and Digital Media, London Metropolitan University, London, UK

Correspondence

Ignacio J. Garcia Zuazola, School of Computing and Digital Media, London Metropolitan University, London N7 8DB, UK.
Email: i.garciazuazola@londonmet.ac.uk

Funding information

Department of Science and Technology, Ministry of Science and Technology, India, Grant/Award Number: ECR/2018/000343

Abstract

A compact, flexible, long-range, and impedance transformer balun-like integrated UHF RFID tag antenna is proposed for the detection of water bottles. To alleviate the performance of a tag antenna in close proximity to a high dielectric material such as water, the radiating element of the tag antenna uses folded, unbalanced strips made of balun-like arms wrapped around the tag's body. As a result, a wide bandwidth with reasonably good radiation resistance is achieved. The tag's body comprises dual loops for the impedance matching to the tag chip. This leads to a long read range of 13.33 m; >5.83 m compared to other state-of-the-art designs. The proposed tag antenna conforms to a small footprint by wrapping the balun-like arms around the tag's body, which results in a compact form. The tag is fabricated, and the results reasonably agree with simulations.

1 | INTRODUCTION

Radio-Frequency Identification (RFID) is perceived as an integral technology for applications such as the Internet of Things (IoT) [1], management of goods and objects [2], healthcare [3], animal tracking [4], electronic toll collection [5], asset identification [6] etc. RFID readers use back-scattering to retrieve the tag's unique identification. The operating frequency band for the UHF RFID is allocated between 840 and 960 MHz worldwide, specifically 865–868 MHz for Europe, New Zealand, and India, 902–928 MHz for USA, 940–943 MHz for China, and 908.5–914 MHz for Korea [7, 8]. Due to its widespread applications, several cost-effective, small, and malleable solutions exist for RFID tags. However, their performance is inherently compromised when attached to water bottles; as a result, the reading range decreases due to low gain and impedance mismatch with the tag chip [9]. Therefore, particularly for applications, such as liquid inventory, the design process of the tags must take into account the permittivity of water [10]. Moreover, a compact, long-range, and flexible tag is preferred to easily attach to naturally curved bottles. This is performed using an efficient conjugate impedance matching technique to match the tag antenna impedance with the RFID chip.

In the literature, several design techniques were reported to improve the tag performance on water bottles. For instance, a T-matching technique was used in Refs. [9, 11–19] to monitor the tag on wine and water bottles. Similarly, a few designs for water levelling and distance monitoring were proposed in Refs. [20, 21], having limited read range with large dimensions. However, the T-matching technique did not provide wide bandwidths. Therefore, to achieve better impedance matching on the liquid-filled bottles, two loops are used. For instance, some tag antennas incorporating a nested slot feed were proposed in Refs. [10, 22–33] to improve impedance matching, however, offering a read range of ~2.5 m. The nested slot technique showed large dimensions [24], with adverse effects in close proximity of water. Similarly, a conformal tag antenna with a reading range of 3.5 m [34, 35] was proposed for a smart blood repository system to track blood bags [36]. Furthermore, RFID tags were proposed for liquids such as, humidity of the soil [37], intravenous (IV) [38], shakes, wine, and orange juice [39]. Similarly, a slot enabled near the body tag was proposed in Ref. [40]. The aforementioned designs have relatively large dimensions, and a few are inflexible with a low read range. Moreover, the water bottle industry employs stacked or piled packing; therefore, mutual coupling occurs between tags, resulting in compromised gain and impedance mismatching. Thus, water bottle monitoring and identification is an issue in dynamic and different environments within the industry. Moreover, a bidirectional tag antenna was proposed in Ref. [41] to reduce the mutual coupling between tags.

Thus, to satisfy the current needs of tag antennas with low footprint but long read range detection of water bottles, a compact, flexible, mutual coupling insensitive UHF RFID balun-like integrated tag antenna for long range detection of water bottles is proposed. This paper comprises six sections. Introduction was reported in Section 1. The problem analysis of conventional designs with the proposed design is presented in Section 2, the simulated results including a parametric study in Section 3, and the fabrication and measurements in Section 4. The paper is concluded in Section 5.

2 | PROPOSED SYSTEM MODEL

The schematic model of the proposed UHF RFID tag antenna for tracking water-filled bottles in commercial industry applications is shown in Figure 1.

Each carton box in the warehouses is filled with $M \times N$ closely packed water bottles, and each bottle is labelled with an RFID tag. Therefore, a bore-sight radiation pattern is not desired for this specific application as the bore-sight affects the tag performance negatively due to mutual coupling with unlikely read tags. Hence, a bi-directional antenna is required to overcome the mentioned issue.

2.1 | Observation and problems in conventional designs

For the evolution of the proposed design, tags with conventional impedance matching techniques were investigated and printed on a single-sided polyester substrate (a label) having $\epsilon_r = 3.2$, $\tan\delta = 0.002$, and thickness 0.1 mm with a copper ink deposition of 10 μm using the commercial electromagnetic software Ansys HFSS. The conventional tags were simulated over a high-density poly ethylene (HDPE) bottle of 1 mm thickness [9] filled with water, as illustrated in Figure 2. This assumed the dielectric constant and electrical conductivity of water (H_2O) as $\epsilon_r = 81$ and $\sigma = 0.01$ S/m, respectively.

Their corresponding current distributions with water are presented in Figure 3. The results using T-matching techniques are illustrated in Figure 3a, which show non-uniform currents in the presence of water. On the other hand, the nested H-shaped slot technique of Figure 3b showed more balanced current distributions with relatively larger dimensions and low gain. To corroborate this in regard to their input reactance, the immediately outlined techniques were simulated at 866 MHz, and their corresponding impedances are presented in Table 1.

It is noted that the reactance of the T-matching and nested H-shaped slot vary significantly in the presence of water from the chip impedance ($Z_c = 38.83 + j153.30$). In addition, similar results are obtained from conventional reported T-matching

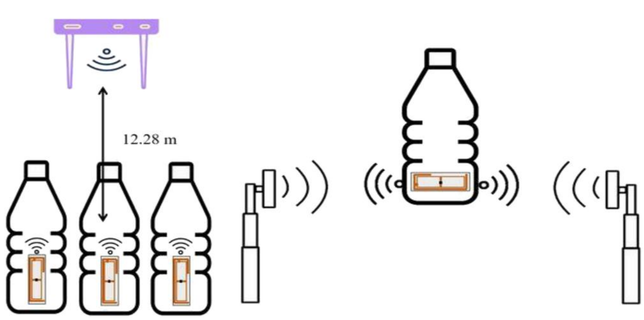

FIGURE 1 Schematic model of the proposed UHF RFID tag for water bottle applications in industry

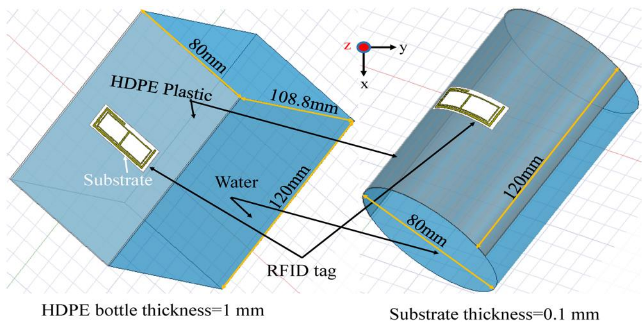

FIGURE 2 Simulation layout of the proposed tag antenna (left) on a container and (right) on a water bottle

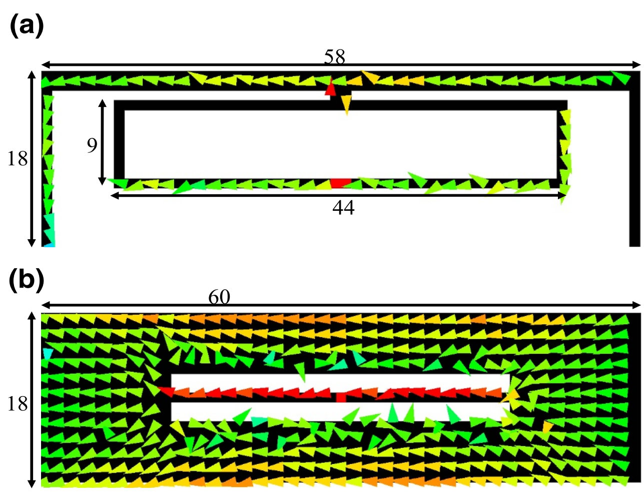

FIGURE 3 Current distributions for (a) T-matching and (b) nested H-shaped slot [42] with a water bottle

TABLE 1 Impedance for the different techniques

Techniques	With water bottle (η_r)	Gain (dBi)
T-matching	62.17 + j237.50 (12%)	−5.5
Nested H-shaped slot	14 + j120.57 (19%)	−2.1

[11, 12] and nested H-shaped slot designs [10, 14, 20, 21, 23] where the reading range of the tags was constrained in the presence of water. The T-matching technique reported a limited bandwidth, and the impedance of the tag antenna varied significantly in the presence of water. Similarly, the nested slot technique has large size radiators, and the radiation efficiency (η_r) of both tags was constrained in the presence of water. The following problems are observed in the conventional UHF RFID tags:

- The impedance changes significantly in the presence of water; therefore, to design an efficient tag antenna, it must be impedance tolerant.
- The efficiency is reduced in the presence of water; therefore, an efficient tag antenna is desired.

Following the immediately mentioned observations, a novel UHF RFID tag antenna is proposed, and its performance in the presence of water is discussed in the next subsection.

2.2 | Design

The dimensions of the proposed tag antenna is shown in Figure 4.

The tag antenna comprises a radiating element using unbalanced strips made of balun-like arms, and these arms were wrapped around the tag's body (the parallel dual loops) to minimise the overall size of the tag. The unbalanced strips led to an optimum design with reasonably good impedance matching, current density, and long read range. The parallel dual loops were used for their relatively good reactive impedance matching on high permittivity (water) compared to other conventional methods; this is achieved by a widespread magnetic field (H-field) distribution in the near-field, which is less affected in the presence of water. The design evolution is presented next.

2.3 | Design evolution

The initial antenna element was designed using the parallel dual loops to obtain a wider bandwidth and relatively good impedance matching on high permittivity (water) in the desired UHF RFID band, as shown in Figure 5.

The dual loops were simulated following the procedure of Figure 2; an input impedance of (22.12 + j136.69) is obtained. The parametric analysis for this is reported later Section 3.1. To satisfy the second condition, in which η_r is to be improved, the radiating arms (unbalanced strips) of the proposed tag antenna were targeted for compactness and then carefully wrapped around the dual loops to minimise the adverse effects of the water. This is in contradiction with conventional approaches where large-size radiators are common.

It is noted that the reactance of the T-matching and nested H-shaped slot vary significantly in the presence of water,

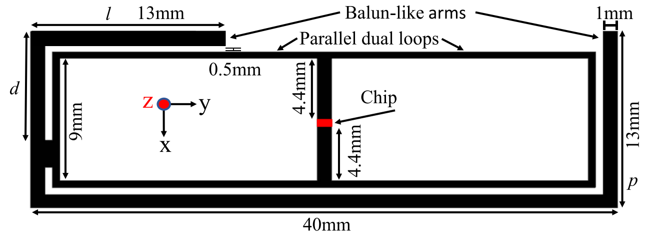

FIGURE 4 Dimensions of the proposed tag antenna

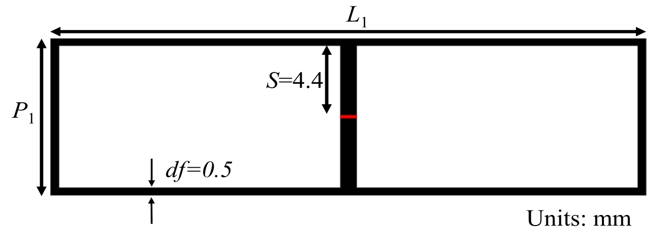

FIGURE 5 Dimensions of the loop antenna

whereas the parallel dual loops with reactance 136.69 Ω offered relatively good conjugate matching with the chip's reactance (−154.31 Ω) when attached to the water bottle. Furthermore, the η_r of the reported designs was ~12%, whereas the proposed tag antenna was 27% in the presence of water. The folded, unbalanced strips of balun-like arms wrapped around the parallel dual loops are presented next.

2.4 | Effect of unbalanced strips

The effect of the unbalanced strips was observed by evaluating the current distributions shown in Figure 6. The differential mode/common mode (DM/CM) was defined by means of the current distribution along the tag antenna. Whereas in the dual loops, a DM was present due to the opposite currents flowing at every point in the loops, in the unbalanced strips, a CM was triggered from currents flowing in an even direction. The effect with the water bottle, depicted in Figure 6a, demonstrated that the currents in the unbalanced strips flowed constructively with the dual loops. This is because the proposed tag antenna (unbalanced strips connected to parallel dual loops) serves as an impedance transforming balun, enabling a DM current in the dual loops and a CM in the unbalanced strips depending on design parameters. To corroborate this, the current distribution of the tag for various lengths of d (defined in Figure 4) are shown in Figure 6a–c, where d defines the location of the joint between the unbalanced strips and the dual loops. For d = 6.6 mm, the current magnitude distribution in the dual loops was non-uniform (Figure 6b); similarly, for d = 8.6 mm (Figure 6c), the DM current distribution existed in the dual loops. However, when d = 7.6 mm (Figure 6a), the desired current distributions in the dual loops and unbalanced strips were found, corroborating the impedance transformer balun-like behaviour. The following input impedances, 38.83 + j153.30, 36.44 + j154.80, and 29.62 + j159.76, were

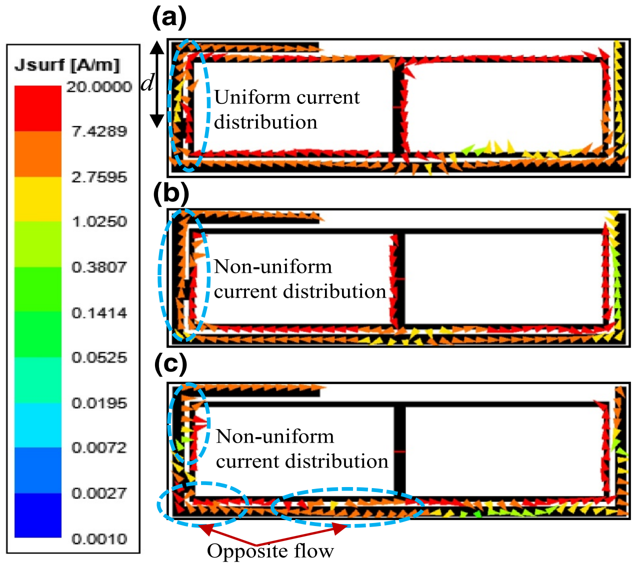

FIGURE 6 Current distributions (a) with a water bottle for d = 7.6 mm, (b) d = 6.6 mm, and (c) d = 8.6 mm

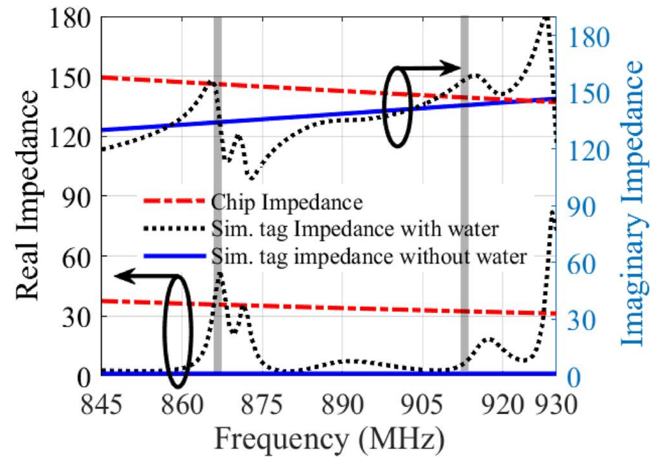

FIGURE 7 Impedance of the proposed tag antenna with and without a water bottle

observed for d = 6.6, 7.6, and 8.6 mm, respectively, proving that out-of-phase currents in the unbalanced strips (balun-like arms) affected the impedance matching of the tag positively.

3 | SIMULATED RESULTS

The proposed tag antenna was simulated to evaluate its input impedance $Z_a = R_a + jX_a$, gain $G_r(\phi, \theta)$, and read range performance by following the procedure of Figure 2. The read range, d, was calculated theoretically using the Friss equation as

$$d = \frac{\lambda}{4\pi}\sqrt{\frac{P_t G_t(\phi,\theta) G_r(\phi,\theta)\tau P_m}{P_{th}}} \tag{1}$$

where P_t is the transmitter power, G_t is the gain of the transmitter antenna, P^{th} is the chip sensitivity (−22.5 dBm), and P_m is the polarisation mismatch efficiency (P_m = 0.5 for the circularly polarised transmitter antenna). Here, τ is the power transmission coefficient and can be calculated as

$$\tau = \frac{4R_c R_a}{|Z_c + Z_a|^2}, 0 \le \tau \le 1 \tag{2}$$

where $Z_c = R_c - jX_c$ is the chip impedance. For the conjugate matching, a 1.13 pF capacitance with a parallel resistance of 0.7 kΩ was assumed for the chip. The impedance matching between the tag antenna and chip was estimated using Equation (2), and the simulated input impedance of the proposed tag antenna with and without a water bottle is illustrated in Figure 7.

Since the antenna was tailored for water applications, it is observed that the impedance of the proposed tag antenna (with water) is well matched to the chip impedance in the ETSI and FCC bands. However, this is not the case when the water is not present. That is a compromised 25% efficiency.

3.1 | Parametric analysis

A parametric study of the unbalanced strips was carried out by varying l and p at 866 MHz to maximise the reading range. The thickness of the water bottle was 1 mm, and the length of l and p were varied in the 1–20 and 1–15 mm ranges, respectively. The maximum reading range of ~13.33 m is shown in Figure 8 when $l = p$ = 13 mm, which corresponds to a simulated gain of 0.2 dBi.

Furthermore, the parametric study of the dual loops (P_1 and L_1 in Figure 5) was conducted to analyse the effects of its dimension on the impedance matching, results are shown in Table 2. The P_1 and L_1 were chosen as 10 and 37, respectively, based on the impedance matching, since other dimensions exhibit significant reactance, which fluctuates more during the integration of unbalanced strips.

3.1.1 | Effect of bottle thickness

The proposed tag antenna was attached to HDPE plastic bottles of different thicknesses (0.3–1.5 mm) to investigate the impact of bottle thickness on the reading range. The result indicates a maximum reading range of 14.30 m achieved for a 1.5 mm bottle thickness and a minimum reading range of 10.19 m for 0.3 mm. This is shown in Table 3.

3.1.2 | Effect of bottle volume

The proposed tag antenna was also investigated for bottles of different volumes filled with water. Table 4 shows the effect for the different cases. Although a compromise performance can be observed for unrealistically small bottle volumes (3.

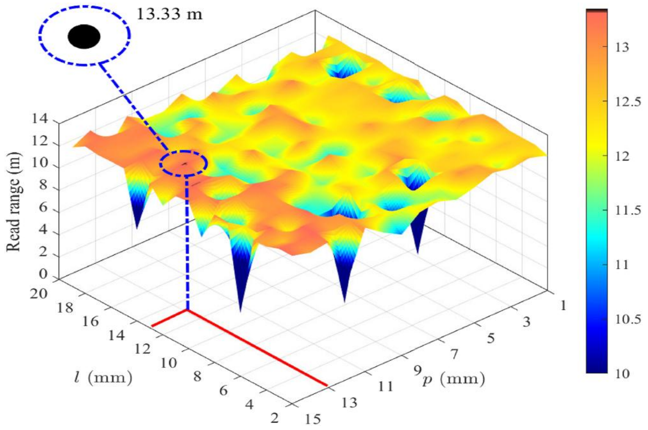

FIGURE 8 Parametric study of the unbalanced strips at 866 MHz for the tag on a water-filled HDPE bottle

TABLE 2 Parametric study of dual-loop impedance at 866 MHz for the tag on a water-filled bottle

S.N.	P_1 (mm)	L_1 (mm)	Impedance (Ω)
1.	9	36	15.24 + j160.12
2.	9	37	3.34 + j123.01
3.	9	38	31.39 + j150.09
4.	10	36	24.87 + j153.26
5.	10	37	22.12 + j136.69
6.	10	38	29.31 + j160.26
7.	11	36	24.62 + j184.98
8.	12	37	43.87 + j169.47
9.	13	38	49.65 + j185.12

and 4.), more prominent results are observed for realistic cases (1. and 2.).

3.1.3 | Effect of different graded bottle

The proposed tag antenna performance was also evaluated for bottles made from various plastic materials such as HDPE, PET, PVC, Polypropylene (PP), and LDPE. Bottle thicknesses of 1 mm were considered for this analysis. Table 5 shows reasonable impedance matching results on various plastic materials with only a slight variation in the reading range.

3.2 | Performance of the proposed tag antenna with frequency

Although the proposed tag antenna was tailored for the 866 and 915 MHz frequency bands, Table 6 shows its behaviour for several frequency bands. A maximum reading range of 13.33 m is achieved in the ETSI band (866 MHz) and a read range of 4.22 m in the lower FCC band (902 MHz).

3.3 | Magnetic field distribution and bending tolerance

The magnetic field (H‐field) distribution of the proposed tag antenna was also simulated and is illustrated in Figure 9. The H‐field was observed in a plane 1 mm away from the tag. It is apparent from Figure 9 that the H‐field intensity is higher within the dual‐loop area. It was witnessed that a large dual loop led to wide H‐field distribution and that, compared to

TABLE 3 Performance of the proposed tag on different thicknesses of the water bottle

S.N.	Bottle‐thickness (mm)	Impedance (Ω)	Gain (dBi)	Reading range (m)
1.	0.3	82.88 + j233.34	0.2	10.19
2.	0.4	54.80 + j183.40	0.5	12.84
3.	0.5	48.56 + j181.66	0.1	12.39
4.	0.7	45.92 + j162.7	0.3	13.31
5.	1	36.44 + j154.8	0.2	13.33
6.	1.2	46.56 + j155.52	0.1	13.06
7.	1.5	39.93 + j144.13	0.9	14.30

TABLE 4 Performance of the proposed tag antenna for various water bottle volumes

S.N.	Volume‐water‐filled bottle (mm^3)	Impedance (Ω)	Gain (dBi)	Reading range (m)
1.	120 × 80 × 108.8	36.44 + j154.8	0.2	13.33
2.	200 × 100 × 120	5.71 + j145.88	0	8.79
3.	80 × 50 × 100	1.92 + j125.60	−5.7	2.36
4.	75 × 50 × 50	2.58 + j136.69	−5.3	3.22

S.N.	Material	Impedance (Ω)	Gain (dBi)	Reading range (m)
1.	HDPE	36.44 + *j*154.8	0.2	13.33
2.	PET	46.52 + *j*165.26	0.6	13.72
3.	PVC	38.6 + *j*159	0.59	13.90
4.	Polypropylene (PP)	33.72 + *j*138.91	0.5	13.46
5.	LDPE	36.81 + *j*156	0.2	13.32

TABLE 5 Performance of the proposed tag antenna on the different grades of the water bottle

TABLE 6 Performance of the proposed tag antenna for in various frequency standards

S.N.	Frequency (MHz)	Frequency allocated	Impedance (Ω)	Gain (dBi)	Reading range (m)
1.	866	Europe/India	36.44 + *j*154.8	0.2	13.33
2.	902	American	1.93 + *j*137.86	−1.9	4.22
3.	908.5	Korea	2.79 + *j*145.30	−1.4	5.59
4.	915	FCC/American	13.26 + *j*158.79	0.3	11.92
5.	928	American	41.15 + *j*186.06	−2.4	9.11

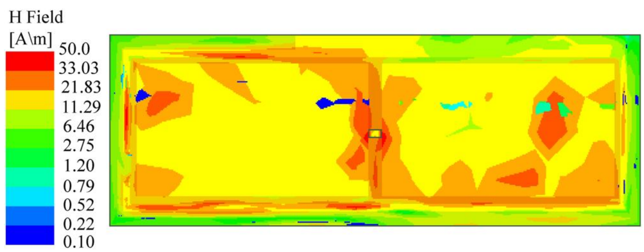

FIGURE 9 H-field distribution of the proposed tag antenna

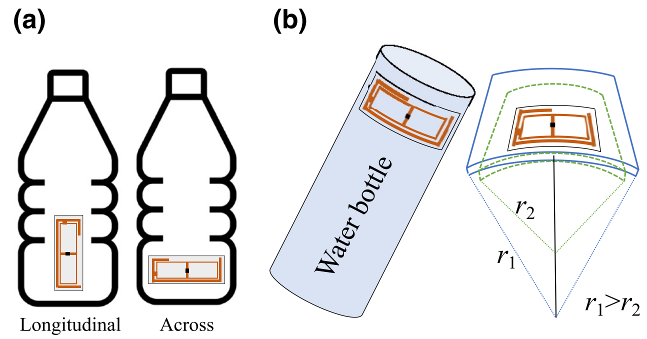

FIGURE 10 The proposed tag (a) affixed on a water bottle and (b) bending tolerance simulation model for different bottle sizes

other conventional methods, significantly improved the read range. The bending tolerance of the proposed tag antenna used as a label was evaluated when affixed on bottles of various shapes. This tag antenna was placed longitudinal or across the length of the water bottle, as shown in Figure 10a. Naturally, the bending was prominent for the latter. Therefore, the read range for different bendings was simulated using the model depicted in Figure 10b, where the bending radius is denoted as r. Note that $r = \infty$ represents a flat surface, whereas lower values of r represent a higher bending corresponding to water bottles of smaller size. The simulated read range of the proposed tag antenna on water bottles of different r is shown in Table 7. A maximum read range of 13.33 and 5.8 m was found for $r = \infty$ and $r = 15$ mm, respectively. Additionally, results revealed that for a typical water bottle of 50 cl having $r = 35$ mm, the proposed tag antenna attained a read range of 12.43 m, which is an acceptable bending tolerance.

TABLE 7 Bending tolerance of the proposed tag on the water bottle

Radius r of bottle (mm)	∞	35	30	25	20	15
Read range (m)	13.33	12.43	10.3	10.1	6.8	5.8

3.4 | Mutual coupling

Mutual coupling can cause a change in the input impedance of tag antennas, resulting in significantly reduced power transfer to the chip. Therefore, especially in systems where several RFID tag antennas must coexist, the mutual coupling should be assessed in order to validate the design. Figure 11 shows the simulation setup, considers two neighbour models, and evaluates the mutual coupling effect by stimulating both tags simultaneously. The response is given in Figure 12 and shows a −30 dB coupling effect between tags, which is reasonable for stockpiling applications.

4 | FABRICATION AND MEASUREMENT

The proposed tag antenna was fabricated, as shown in Figure 13a, by a screen printing process, which involved a transfer of copper ink onto a single-sided polyester (typical

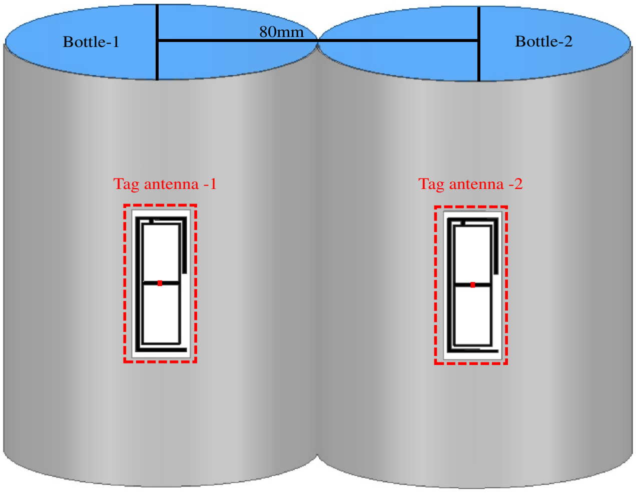

FIGURE 11 Simulation of two neighbouring proposed tag antennas

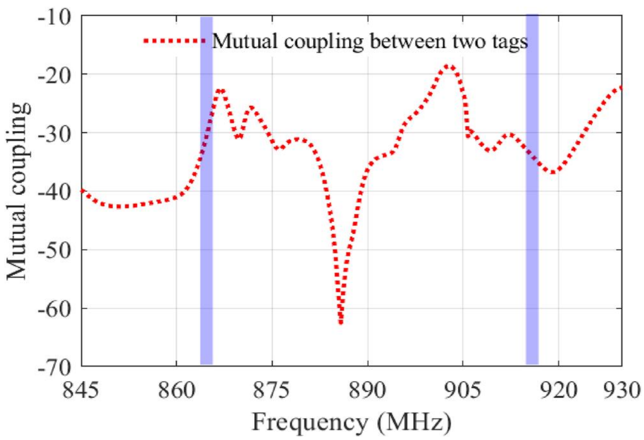

FIGURE 12 Mutual coupling between two neighbouring proposed tag antennas

label of a bottle of water) whose material properties were earlier detailed in Section 2.1.

The tag antenna (used as a label) was then affixed on a water bottle. The measurement setup is shown in Figure 13b, which includes a 9 dBi transmitter horn antenna fed with an RF signal generator (Agilent Technologies) and a Keysight N9915 A handheld spectrum analyser (SA) connected to the proposed tag antenna for measuring received power. A matching circuit was employed for the experiments when connected to the Spectrum Analyser (SA); the associated insertion loss (IL) was accounted for. The measurement is accurate enough since the SA is a narrow band with a lower noise floor and better dynamic range, so its sensitivity is better than traditional power metres. The signal generator was set at 27 dBm, and the received signal strength was measured using the SA. The measurements were performed for the ETSI (866 MHz) and FCC (915 MHz) bands. It was witnessed that the proposed tag antenna had better signal strength compared to that in the literature. The maximum received signal strength reported in the literature is −50 dBm, compared to the

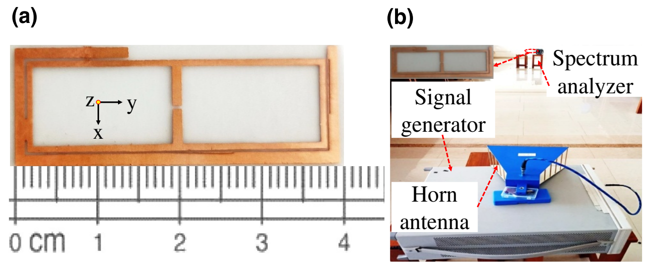

FIGURE 13 (a) Fabricated and (b) measurement setup of the proposed tag antenna

TABLE 8 Measured and simulated impedance of the proposed tag antenna

Frequency (MHz)	Measured	Simulated
866	23.17 + j137.03 Ω	36.44 + j154.8 Ω
915	20.5 + j136.07 Ω	13.26 + j158.79 Ω

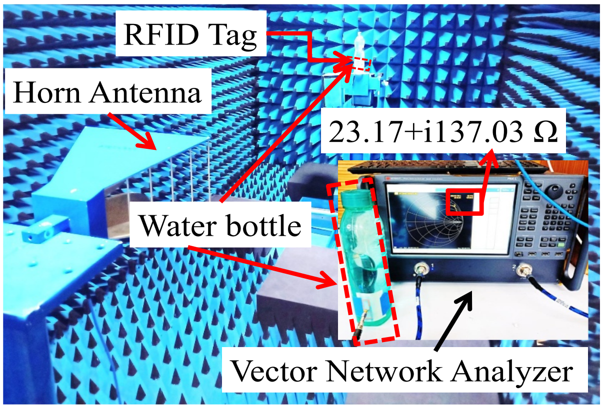

FIGURE 14 Measurement setup of the proposed tag antenna with a water bottle

proposed tag of −19 dBm; both measured 12 m away from the transmitter using the ETSI band. The proposed tag antenna was affixed to the water bottle for realistic measurements and moved carefully closer to the transmitter until a minimum of −19 dBm at 866 MHz and −20 dBm at 915 MHz was attained, which led to a read range of 12.28 and 11.13 m for the ETSI and FCC bands, respectively.

4.1 | Impedance measurement

A two-port S-parameter approach [43] is used to calculate the input impedance of the tag antenna, which transforms the S-parameter into Z-parameters. The tag antenna is regarded as a two-port network in this approach, and the differential impedance is calculated using Equation (3). Two semi-rigid coaxial cables and a Keysight PNA-L were required to perform the S-parameter measurements.

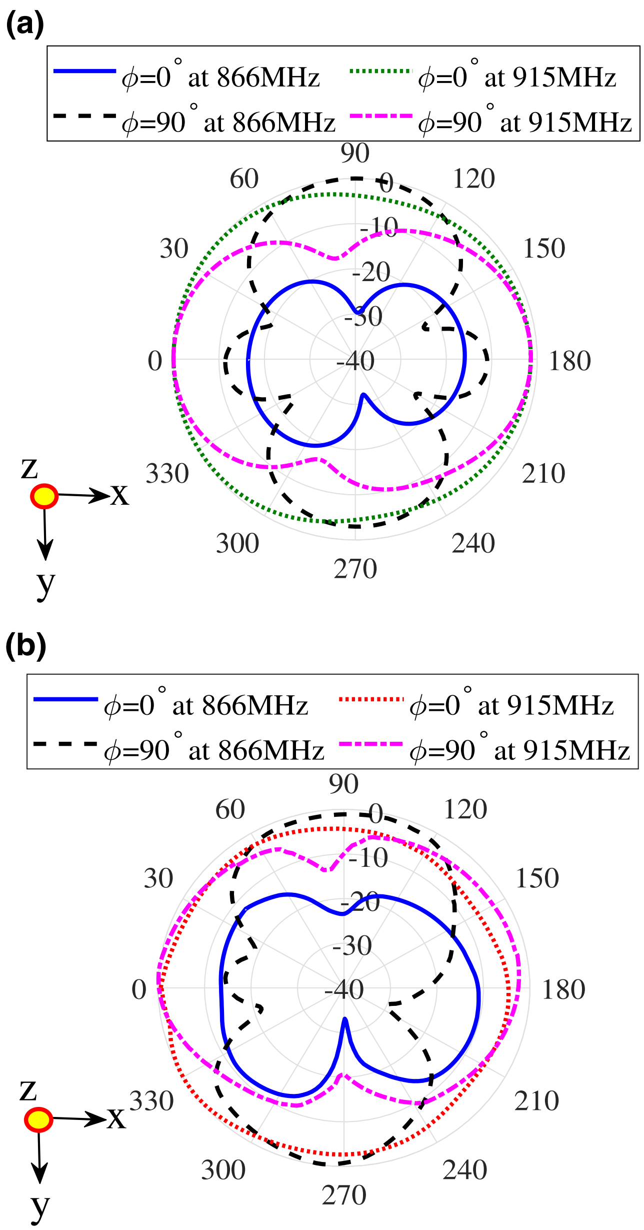

FIGURE 15 (a) Simulated and (b) measured radiation patterns of the proposed tag on a water-filled HDPE bottle

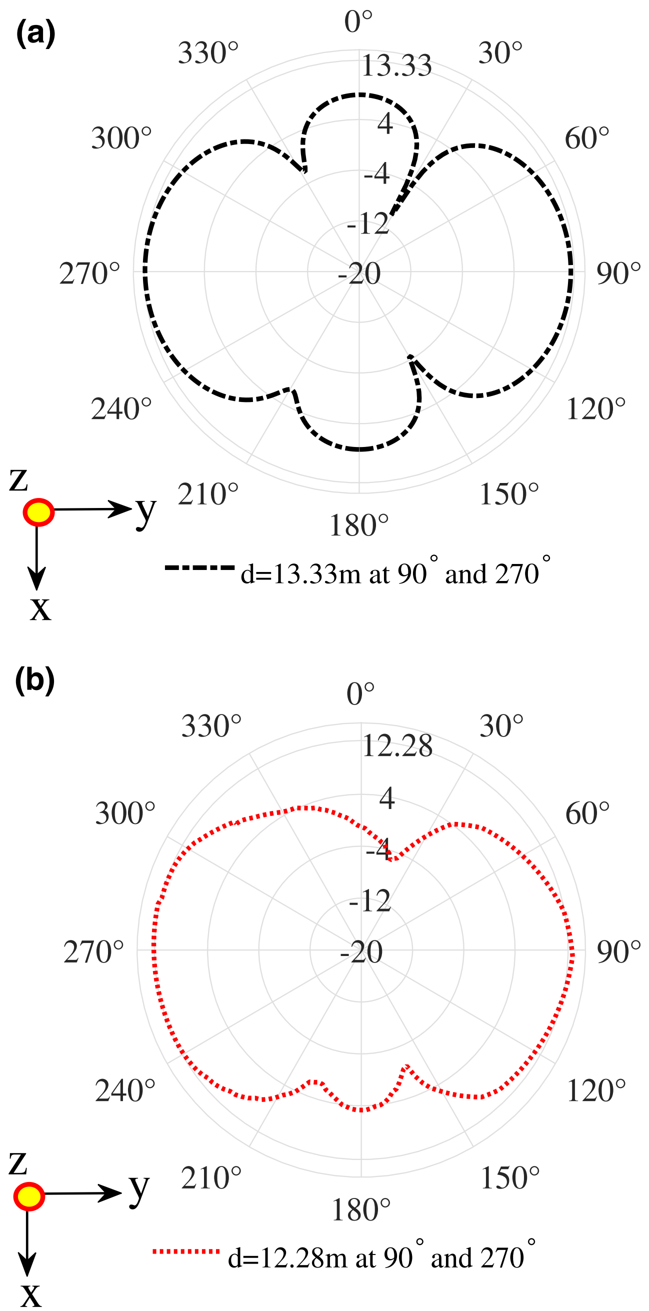

FIGURE 16 (a) Simulated and (b) measured read range patterns of the proposed tag on a water-filled HDPE bottle

$$Z_t = \frac{2\ Z_0(1 - S_{11}S_{22}) + (S_{12}S_{21}) - S_{12} - S_{21}}{(1 - S_{11})(1 - S_{22}) - S_{12}S_{21}} \quad (3)$$

The Vector Network Analyser (VNA) was carefully calibrated to obtain accurate S-parameters, and the effects of the semi-rigid coaxial cables were compensated using the port extension technique. The measured and simulated impedance of the proposed tag antenna with a water bottle at 866 and 915 MHz are listed in Table 8. The theoretical chip impedance $35.58 - j154.31\ \Omega$ at 866 MHz and $32.28 - j146.83\ \Omega$ at 915 MHz is also provided for reference. The simulated and measured findings indicate similar trends; however, certain inconsistencies between the simulated and measured results were due to the manufacturing tolerances and some variation in water and HDPE bottle properties, which led to a slight deviation of the measured input impedance of the fabricated tag antenna from simulations.

4.2 | Radiation pattern measurement

The radiation patterns of the proposed tag antenna (with water bottle) were measured in an anechoic chamber (Figure 14) and the results are shown in Figure 15.

TABLE 9 Comparison with state-of-the-art designs

Reference	Substrate	Size (mm)	Measured read range (m) at 866 MHz	Flexible	Miniature	Long-range (≥4 m)
[9]	Polyester	86 × 22.5 × 0.05	2.2	Yes	No	No
[10]	FR4	81 × 23 × 1.5	2.5	No	No	No
[11]	Paper	40 × 20 × 0.02	~0.34	Yes	Yes	No
[15]	Rogers Ultralam 3850HT	28 × 13 × 0.35	2.51	Yes	Yes	No
[24]	F4B-2	76 × 32 × 0.8	10	No	No	Yes
[25]	Polyimide	44 × 20 × 0.2	1.45–5.6	Yes	Yes	Yes
[34]	Polyester	87.8 × 57.9 × 0.05	4.25	Yes	No	Yes
[35]	Plastic	87.8 × 57.9 × 0.125	4	Yes	No	Yes
[37]	FR4	115 × 40 × 0.5	7.5	No	No	Yes
[39]	Silicon	70 × 30 × 3	1.9–2.5	Yes	No	No
This work	Polyester	40 × 13 × 0.1	12.28	Yes	Yes	Yes

The bidirectional patterns, more apparent at 866 MHz, are perceived as positive for bottling lines applications where a reduction of the mutual coupling [41] among tagged water bottles in closely stacked or piled packing is expected in the bottled water industry. The maximum measured gain of the proposed tag antenna (with water bottle) was 0.05 dBi and −0.6 dBi at 866 and 915 MHz, respectively. Although the proposed tag antenna was specifically designed for the 866 MHz band, results are shown additionally at 915 MHz to demonstrate its performance in the FCC band. Further, the reading range of the proposed tag antenna measured at various angles (0°–360°) was evaluated and is presented in Figure 16. The simulated result is also included in the figure and show reasonable agreement between both (Figure 16a, b). Because the read range patterns are more bidirectional-like, this is attractive for water inventory in industrial applications, such as a conveyor belt, and stockpiling where mutual coupling minimal effect (0° and 180°) is preferred.

4.3 | Performance comparison

Table 9 includes various state-of-the-art designs widely available in the literature for comparison, showing the proposed tag antenna (affixed to a water bottle), a longer read range, and a smaller footprint (miniature design) compared to other designs. For instance, although Ref. [25] is only 4 × 7 × 0.1 mm bigger than the proposed counterpart, it offers a 6.68 m lowered read range. Furthermore, a multi-slot tag antenna with a 36 × 19 × 0.7 mm bigger size and a 2.28 m lower reading range was proposed in Ref. [24]. Similarly, Ref. [37] offers a lowered 4.78 m read range and 75 × 27 × 0.4 mm bigger size. This corroborates the out performance of the proposed tag antenna in terms of compact size and long read range.

5 | CONCLUSION

This paper presents a compact, flexible, mutual coupling insensitive UHF RFID impedance transformer balun-like integrated tag antenna for long-range water bottle detection. The tag antenna comprised folded, unbalanced strips made of balun-like arms wrapped around the tag's body. The proposed tag showed good impedance matching between the antenna and the chip and an outstanding read range compared to other state-of-the-art designs, bringing a compact tag with a long detection range in liquid inventory RFID applications. The tag was found to be 12–50% smaller in size with a >5.83 m longer read range compared to other state-of-the-art designs.

ACKNOWLEDGEMENTS

This work was supported by SERB, Department of Science & Technology, Government of India, under Grant ECR/2018/000343.

CONFLICT OF INTEREST

The author declares that there is no conflict of interest that could be perceived as prejudicing the impartiality of the research reported.

DATA AVAILABILITY STATEMENT

The data that support the findings of this study are available from the corresponding author upon reasonable request.

ORCID

Manoj Garg https://orcid.org/0000-0003-4196-2444

REFERENCES

1. Lizzi, L., Ferrero, F.: Use of ultra-narrow band miniature antennas for Internet-of-Things applications. Electron. Lett. 51(24), 1964–1966 (2015). https://doi.org/10.1049/el.2015.3142

2. Kumar, M., Sharma, A., Garcia Zuazola, I.J.: All-in-one UHF RFID tag antenna for retail garments using nonuniform meandered lines. Prog. Electromagn. Res. Lett. 94, 133–139 (2020). https://doi.org/10.2528/pierl20072102
3. Sharma, B., Koundal, D.: Cattle health monitoring system using wireless sensor network: a survey from innovation perspective. IET Wirel. Sens. Syst. 8(4), 143–151 (2018). https://doi.org/10.1049/iet-wss.2017.0060
4. Siegel, P.H.: Microwaves are everywhere: RFID-do you know where your pet is? IEEE J Microw. 1(3), 679–688 (2021). https://doi.org/10.1109/jmw.2021.3081022
5. Chao, C.-P., et al.: Novel UHF RFID tag antenna design for electronic toll collection. In: 2021 IEEE International Symposium on Radio-Frequency Integration Technology (RFIT), pp. 1–3 (2021)
6. Kumar, M., Sharma, A., Garcia Zuazola, I.J.: A biodegradable multi-platform tolerant passive UHF RFID tag antenna for short-life cycle IoT applications. In: 2021 IEEE Indian Conference on Antennas and Propagation (InCAP), pp. 391–394 (2021)
7. Abdelrahim, W., Feng, Q.: Compact broadband dual-band circularly polarised antenna for universal UHF RFID handheld reader and GPS applications. IET Microw. Antenn. Propag. 13(10), 1664–1670 (2019). https://doi.org/10.1049/iet-map.2018.5970
8. Kumar, M., Sharma, A., Garcia Zuazola, I.J.: Bendable ultra-high frequency radio-frequency identification tag antenna for retail garments using nonuniform meandered lines. Eng. Rep. 3, 1–11 (2021). https://doi.org/10.1002/eng2.12420
9. Sohrab, A.P., et al.: A UHF RFID tag with improved performance on liquid bottles. IEEE Antenn. Wireless. Propag. Lett. 15, 1673–1676 (2016). https://doi.org/10.1109/lawp.2016.2521786
10. Dubok, A., Smolders, A.B.: Miniaturization of robust UHF RFID antennas for use on perishable goods and human bodies. IEEE Antenn. Wireless. Propag. Lett. 13, 1321–1324 (2014). https://doi.org/10.1109/lawp.2014.2337051
11. Zhao, Z., et al.: Compact UHF RFID tag antenna for platform tolerant applications. In: 2018 International Conference on Microwave and Millimeter Wave Technology (ICMMT), pp. 1–3 (2018)
12. Deleruyelle, T., et al.: An RFID tag antenna tolerant to mounting on materials. IEEE Antenn. Propag. Mag. 52(4), 14–19 (2010). https://doi.org/10.1109/map.2010.5638229
13. Xi, J., Ye, T.T.: Conformal UHF RFID tag antenna mountable on winebottle neck. In: Proceedings of the 2012 IEEE International Symposium on Antennas and Propagation, pp. 1–2 (2012)
14. Aroor, S.R., Deavours, D.D.: Evaluation of the state of passive UHF RFID: an experimental approach. IEEE Syst. J. 1(2), 168–176 (2007). https://doi.org/10.1109/jsyst.2007.909179
15. Carlos, D., et al.: Ultra slim and small UHF RFID tag design for mounting on curved surfaces. AEU Int. J. Electr. Commun. 128, 153502 (2021). ISSN 1434-8411. https://doi.org/10.1016/j.aeue.2020.153502
16. Gonçalves, R., et al.: UHF RFID tag antenna for bottle labeling. In: 2014 IEEE Antennas and Propagation Society International Symposium (APSURSI), pp. 1520–1521 (2014)
17. Gonçalves, R., et al.: RFID tags on cork stoppers for bottle identification. In: 2014 IEEE MTT-S International Microwave Symposium (IMS2014), pp. 1–4 (2014)
18. Gonçalves, R., et al.: RFID passive tag antenna for cork bottle stopper. In: 2014 IEEE Antennas and Propagation Society International Symposium (APSURSI), pp. 1518–1519 (2014)
19. Kim, Y.: Design of near omnidirectional UHF RFID tag with one-off seal function for liquid bottles. Microw. Opt. Technol. Lett. 55(2), 375–379 (2013). https://doi.org/10.1002/mop.27285
20. Caccami, M.C., Marrocco, G.: Electromagnetic modeling of self-tuning RFID sensor antennas in linear and nonlinear regimes. IEEE Trans. Antenn. Propag. 66(6), 2779–2787 (2018). https://doi.org/10.1109/tap.2018.2820322
21. Görtschacher, L.J., Grosinger, J.: UHF RFID sensor system using tag signal patterns: prototype system. IEEE Antenn. Wireless Propag. Lett. 18(10), 2209–2213 (2019). https://doi.org/10.1109/lawp.2019.2940336
22. Sharif, A., et al.: Low-cost inkjet-printed RFID tag antenna design for remote healthcare applications. IEEE J. Electromag., RF Microw. Med. Biol. 3(4), 261–268 (2019). https://doi.org/10.1109/jerm.2019.2924823
23. Kim, D., Yeo, J.: Low-profile RFID tag antenna using compact AMC substrate for metallic objects. IEEE Antenn. Wireless Propag. Lett. 7, 718–720 (2008). https://doi.org/10.1109/lawp.2008.2000813
24. Tang, T., et al.: Design and radiation mechanism analysis of a multi-usage ultra-high frequency radio frequency identification tag antenna. IET Microw. Antenn. Propag. 13(12), 1989–1996 (2019). https://doi.org/10.1049/iet-map.2018.5789
25. He, S., et al.: High performance UHF RFID tag antennas on liquid-filled bottles. Prog. Electromagn. Res. 165, 83–92 (2019). https://doi.org/10.2528/pier19041001
26. Ouyang, J., et al.: Small conformal UHF RFID tag antenna for labelling fruits. In: 2019 IEEE Asia-Pacific Microwave Conference (APMC), pp. 33–35 (2019)
27. Li, L., He, W.: Anti-water UHF RFID tag antenna with multi-loop structure for impedance matching. In: 2018 Progress in Electromagnetics Research Symposium (PIERS-Toyama), pp. 1805–1808 (2018)
28. Sharif, A., et al.: Low cost conformal UHF RFID tag antenna for plastic water bottles. In: 2018 IEEE International Symposium on Antennas and Propagation & USNC/URSI National Radio Science Meeting, pp. 693–694 (2018)
29. Sharif, A., et al.: Inkjet printed UHF RFID tag based system for salinity and sugar detection. Microw. Opt. Technol. Lett. 61(9), 2161–2168 (2019). https://doi.org/10.1002/mop.31863
30. Lin, D.-B., Tang, I.-T., Wang, C.-C.: UHF RFID H-shaped tag antenna using microstrip feed design on metallic objects. J. Electromagn. Waves Appl. 25(13), 1828–1839 (2011). https://doi.org/10.1163/156939311797454024
31. Amin, Y., et al.: Performance-optimized quadrate bowtie RFID antennas for cost-effective and eco-friendly industrial applications. Prog. Electromagn. Res. 126, 49–64 (2012). https://doi.org/10.2528/pier12020805
32. Aslam, B., et al.: A low profile miniature RFID tag antenna dedicated to IoT applications. Electromagnetics 39(6), 393–406 (2019). https://doi.org/10.1080/02726343.2019.1641654
33. Santiago, A.G., Fernandes, C.A., Costa, J.R.: Broadband UHF RFID passive tag antenna for near-body operation. In: 2012 IEEE International Conference on RFID-Technologies and Applications (RFID-TA), pp. 271–274 (2012)
34. Bjorninen, T., Elsherbeni, A.Z., Ukkonen, L.: Low-Profile conformal UHF RFID tag antenna for integration with water bottles. IEEE Antenn. Wireless Propag. Lett. 10, 1147–1150 (2011). https://doi.org/10.1109/lawp.2011.2171911
35. Bjorninen, T., et al.: Development of a low profile conformal UHF RFID tag antenna for identification of water bottles. In: 2011 IEEE International Symposium on Antennas and Propagation (APSURSI), pp. 533–536 (2011)
36. Zaric, A., et al.: RFID-based smart blood stock system [education column]. IEEE Antenn. Propag. Mag. 57(2), 54–65 (2015). https://doi.org/10.1109/map.2015.2420491
37. Alonso, D., et al.: UHF passive RFID-based sensor-less system to detect humidity for irrigation monitoring. Microw. Opt. Technol. Lett. 59(7), 1709–1715 (2017). https://doi.org/10.1002/mop.30611
38. Ting, S.-H., Wu, C.-K., Luo, C.-H.: Design of dual mode RFID antenna for inventory management and IV fluid level warning system. Int. J. Antenn. Propag. 4, 1–8 (2017). https://doi.org/10.1155/2017/2470291
39. Liu, Q., Li, H., Yu, Y.-F.: A versatile flexible UHF RFID tag for glass bottle labelling in self-service stores. IEEE Access 6, 59065–59073 (2018). https://doi.org/10.1109/access.2018.2874428

40. Santiago, A.G., Costa, J.R., Fernandes, C.A.: Broadband UHF RFID passive tag antenna for near-body applications. IEEE Antenn. Wireless Propag. Lett. 12, 136–139 (2013). https://doi.org/10.1109/lawp.2013.2243400
41. Li, M., Niu, Z., Wang, Y.: An electrically small antenna with a bidirectional radiation pattern for UHF RFID tags. In: 2018 International Conference on Microwave and Millimeter Wave Technology (ICMMT), pp. 1–3 (2018)
42. Sharif, A., et al.: Making assembly line in supply chain robust and secure using UHF RFID. Sci. Rep. 11, 1–17 (2021). https://doi.org/10.1038/s41598-021-97598-5
43. Qing, X., Goh, C.K., Chen, Z.N.: Impedance characterization of RFID tag antennas and application in tag co-design. IEEE Trans. Microw. Theor. Tech. 57(5), 1268–1274 (2009). https://doi.org/10.1109/tmtt.2009.2017288

How to cite this article: Garg, M., et al.: Compact UHF RFID balun-like integrated tag antenna for long range detection of water bottles. IET Microw. Antennas Propag. 17(12), 909–919 (2023). https://doi.org/10.1049/mia2.12299